

and E-Ni Foo, Phys. Rev. **172**, 689 (1969).

<sup>20</sup>P. W. Anderson, Phys. Rev. **100**, 749 (1955).

<sup>21</sup>I. B. Bernstein, Phys. Rev. **109**, 10 (1958).

<sup>22</sup>C. K. N. Patel and R. F. Slusher, Phys. Rev. Letters **21**, 1593 (1968).

<sup>23</sup>Band parameters employed in the calculation are as

follows:  $m_1=0.0011$ ,  $m_2=1.70$ ,  $m_3=0.0301$ ,  $m_4=0.177$ ,  $M_1=0.700$ ,  $M_3=0.063$ , carrier density  $=2.9 \times 10^{17} \text{ cm}^{-3}$ , and Fermi energy of holes  $=11.45 \text{ meV}$ .

<sup>24</sup>The calculations were carried out using an NEAC 2200 at Computer Center of Osaka University.

## Phenomenological Molecular-Field Theory of the Mott-Wigner Transition in Magnetite

J. B. Sokoloff

*Northeastern University, Boston, Massachusetts 02115*

(Received 13 July 1970; revised manuscript received 17 August 1970)

The measurement by Verwey and Haayman of the variation of the transition temperature of magnetite with stoichiometry is discussed in terms of the molecular-field solution of a lattice-gas model of the Mott-Wigner insulator-to-metal transition. This model gives rise to a second-order phase transition. The observed first-order transition is reproduced by substituting a phenomenologically screened interaction, in which the dielectric constant causing the screening decreases with increasing order parameter. Since the phenomenological screening necessary to produce the observed results is very large compared to that expected on the basis of electronic screening, we postulate that the dielectric constant includes the effect of local charge polarization accompanying the ordering. It is possible to obtain a consistent picture of many of the experimental data on magnetite using this model. Inelastic neutron scattering and optical absorption are discussed as means of observing the elementary excitations of the system and to deduce some of the parameters in the theory. The low-lying excitations in the ordered (i.e., insulating) state are shown to be excitons with flat dispersion (i.e., their energies do not depend on wave vector); their energies and cross sections are calculated.

### I. INTRODUCTION

It was suggested by Mott<sup>1,2</sup> that the insulating state of magnetite could be described by a Wigner electron lattice,<sup>3</sup> and the insulator-to-metal transition as a melting of this lattice. Objection was raised to this picture by Rosencwaig<sup>4</sup> because it predicted an increase in the transition temperature as the number of electrons in the system is decreased, instead of the decrease that is actually observed.<sup>5</sup> In Secs. II and III, the insulator-to-metal transition in magnetite is described using a lattice-gas model, which is similar to the molecular-field solution of the Ising model of antiferromagnetism. The model is found to agree qualitatively with the results of Verwey and Haayman on the variation of transition temperature with stoichiometry. The introduction of a phenomenological interaction which varies rapidly with the number of free carriers in the system (and hence with the order parameter) makes it possible to reproduce the observed first-order transition. The behavior of the specific heat and conductivity near the transition temperature is discussed in terms of this effective-interaction version of the lattice-gas model. In Sec. IV, the elementary excitation spectrum, as well as the inelastic-neutron-scattering

and infrared-optical-absorption cross sections, is found. The low-lying excitations are found to be excitons with flat wave-vector-independent bands, and their energy spectrum is calculated. Measurement of the exciton energies would make it possible to deduce some of the parameters in the theory of Secs. II and III.

This model is similar to a model introduced by Cullen and Callen<sup>6</sup> to describe magnetite in that both models introduce a temperature-dependent order parameter to describe the phase transition. Cullen and Callen's model is a Hartree-Fock-approximation energy-band model. The present model leaves out all discussion of details of the electronic energy states, since it is not known as yet whether band theory or small-polaron hopping is a better description of magnetite. The band theoretic description of the problem of Ref. 6 is introduced in Sec. III, however, to describe the pressure dependence of the transition temperature. The treatment presented here shows how the dependence of transition temperature on stoichiometry can be explained using an electron-lattice model. With the phenomenological interaction introduced later, the model is shown to allow a simple and consistent interpretation of much of the experimental data on magnetite using a few simple param-

eters. These are the main contributions of this paper.

In the spinel-lattice structure of magnetite, there are two types of lattice sites containing metallic ions, sites with octahedral and sites with tetrahedral bonding.<sup>7,8</sup> In magnetite, all the tetrahedral sites and half of the octahedral sites are occupied by  $\text{Fe}^{+3}$  ions, and the remainder of the octahedral sites are occupied by  $\text{Fe}^{+2}$  ions. Below the transition temperature, the  $\text{Fe}^{+3}$  and  $\text{Fe}^{+2}$  ions on the octahedral sites are ordered in alternate rows which are perpendicular to each other and perpendicular to the  $c$  axis. That is, as we move along the  $c$  axis we encounter alternate planes of rows of  $\text{Fe}^{+2}$  and  $\text{Fe}^{+3}$  ions<sup>7,8</sup> which are perpendicular. This is illustrated in Fig. 1. Above the transition temperature, these two ions are randomly distributed over the lattice of octahedral sites. It is generally accepted that it is the motion of the extra electron which resides on the  $\text{Fe}^{+2}$  ions (making them  $\text{Fe}^{+2}$  rather than  $\text{Fe}^{+3}$  ions) which gives rise to the electrical conductivity. Magnetite is a ferromagnet; all its octahedral sites have their spin pointing in one direction and all the tetrahedral sites in the opposite direction. Thus, the net magnetization is due to the  $\text{Fe}^{+2}$  ions alone. Since the Néel temperature is around 800 °K, near the Mott-Wigner transition temperature of 119 °K, the spins are just about completely ordered. We will, therefore, assume throughout this discussion that the octahedral sites all have their atomic spins pointed in the same direction. Therefore, to consider the charge ordering of the octahedral-site ions (i.e., of the extra electrons), it is sufficient to consider the motion of spinless extra electrons over the octahedral sites only. (They are spinless because they are constrained to have the same spin.) The remaining 3d electrons on the octahedral sites have spins opposite that of the extra electron, and hence, need not be considered in our discussion.<sup>6</sup>

## II. LATTICE-GAS MODEL OF MOTT-WIGNER TRANSITION

We begin the discussion with the typical lattice-gas model based on the Ising-model Hamiltonian

$$\mathcal{H} = \frac{1}{2} \sum_{ij} J(\vec{R}_i - \vec{R}_j) \Delta_i \Delta_j, \quad (1)$$

where  $\Delta_i$  takes on the values  $\pm 1$  and  $J(\vec{R}_i - \vec{R}_j)$  is the interaction between electrons on sites  $i$  and  $j$ .<sup>9</sup> Here,  $\Delta_i = 2n_i - 1$ , where  $n_i$  is the number of extra electrons on site  $i$ . Then,  $\Delta_i = +1$  means that site  $i$  is occupied by an extra electron (i.e., is an  $\text{Fe}^{+3}$  site), and  $\Delta_i = -1$  means that site  $i$  is not occupied by an extra electron (i.e., is an  $\text{Fe}^{+2}$  site). The sum over  $i$  and  $j$  is taken over octahedral sites only. We neglect kinetic energy or hopping energy in this model. We will see later that this is not a

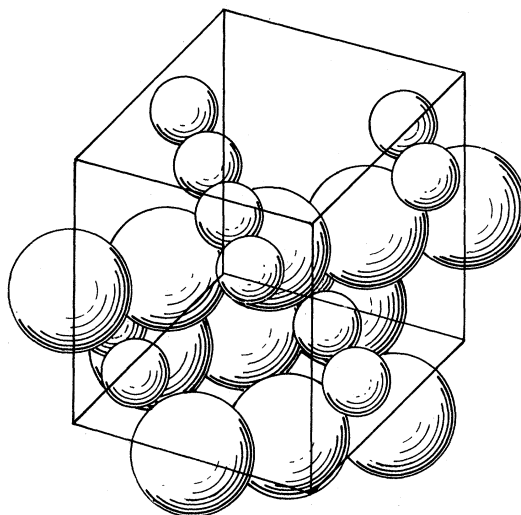


FIG. 1. Octahedral sites in magnetite. [This figure is copied from W. C. Hamilton, Phys. Rev. **110**, 1050 (1958), with the permission of the author.] Large balls represent  $\text{Fe}^{+2}$  ions and the small balls represent  $\text{Fe}^{+3}$  ions.

bad approximation, as experiments indicate that the interaction is probably much greater than the kinetic or hopping energy.

In the molecular-field approximation, Eq. (1) is replaced by

$$\mathcal{H}' = \sum_{ij} J(\vec{R}_i - \vec{R}_j) M_j \Delta_i - \sum_i (H + H' e^{i\vec{Q} \cdot \vec{R}_i}) \Delta_i, \quad (2)$$

where  $M_j$  is the thermal average of  $\Delta_j$ . Here we have included a field  $H$  and a staggered field  $H'$ . (Wave vector  $\vec{Q}$  is along the  $c$  axis and has magnitude  $\pi/c$ , where  $c$  is the spacing along the  $c$  axis between adjacent planes of octahedral sites.) Let us look for a solution for  $M_j$  of the form

$$M_j = M + M' e^{i\vec{Q} \cdot \vec{R}_j}, \quad (3)$$

i.e.,  $M_j$  takes on values  $\frac{1}{2}(M \pm M')$  on alternate planes of octahedral sites as we move along the  $c$  axis. With this assumption, Eq. (2) becomes

$$\begin{aligned} \mathcal{H}' = & [J(0)M - J(\vec{Q})M' - H - H'] \sum_i \Delta_i \\ & + [J(0)M + J(\vec{Q})M' - H + H'] \sum_i \Delta_{i+c}, \end{aligned} \quad (4)$$

where  $-J(\vec{Q})$  is the Fourier transform of  $J(\vec{R})$ , the prime on the summation means that  $i$  is only summed over octahedral planes of  $\text{Fe}^{+2}$  sites, and  $i+c$  signifies that  $i$  has been translated to an adjacent plane of  $\text{Fe}^{+3}$  sites. The partition function is found from Eq. (4) to be

$$\begin{aligned} Z = \text{Tre}^{-\beta \mathcal{H}'} = & \{ \cosh \beta [J(0)M - J(\vec{Q})M' - H - H'] \\ & \times \cosh \beta [J(0)M + J(\vec{Q})M' - H + H'] \}^{N/2}. \end{aligned} \quad (5)$$

Using

$$M = -\frac{KT}{N} \frac{\partial \ln Z}{\partial H},$$

$$M' = -\frac{KT}{N} \frac{\partial \ln Z}{\partial H'} \bigg|_{H'=0},$$

and setting  $H_m = -J(0)M + H$ , we find

$$M' = \frac{1}{2} \{ \tanh \beta [J(\vec{Q})M' + H_m] + \tanh \beta [J(\vec{Q})M' - H_m] \}, \quad (6a)$$

$$M = \frac{1}{2} \{ \tanh \beta [J(\vec{Q})M' + H_m] - \tanh \beta [J(\vec{Q})M' - H_m] \}, \quad (6b)$$

where  $M'$  is the order parameter, the difference between the mean number of extra electrons on alternate rows per lattice site,  $M$  is twice the difference between the mean total number of electrons per site and 0.5 (the value when there is perfect stoichiometry), and  $H_m$  acts as a chemical potential. For  $H_m$  equal to zero,  $M$  is equal to zero, and  $M'$  is nonzero for temperatures below  $T_c^0$ , where

$$kT_c^0 = J(\vec{Q}). \quad (7)$$

When  $T$  reaches this temperature from below, the electron lattice will "melt." The quantity  $M$  is a "stoichiometry parameter," giving the percentage difference in number of electrons in the system from perfect stoichiometry. The  $M$  equal to zero case corresponds to perfect stoichiometry (i.e., half as many extra electrons as sites).

Let us now compare the lattice-gas model with the model of Ref. 6. In the Hartree-Fock band model of Cullen and Callen,<sup>6</sup> the self-consistency condition for the order parameter  $M'$  is given in our notation by

$$1 = \frac{1}{N} \sum_{\vec{k}} \left( \frac{1}{1 + e^{\beta[\epsilon(\vec{k}) - \mu]}} - \frac{1}{1 + e^{\beta[E(\vec{k}) - \mu]}} \right) \frac{1}{E(\vec{k})}, \quad (8)$$

where  $\vec{k}$  is summed over the reduced Brillouin zone introduced in Ref. 6 and where

$$E(\vec{k}) = \left\{ \frac{1}{4} [\epsilon(\vec{k}) - \epsilon(\vec{k} + \vec{Q})]^2 + J(\vec{Q})^2 M'^2 \right\}^{1/2}, \quad (9)$$

where  $\epsilon(\vec{k})$  is the one-electron energy and  $\mu$  is the chemical potential. In the limit  $\epsilon(\vec{k})/J(\vec{Q}) \rightarrow 0$ , Eq. (9) reduces to Eq. (6a) if we identify  $\mu$  with  $H_m$ . Since in the model of Cullen and Callen, the average number of electrons per lattice site  $n$  is given by

$$n = \frac{1}{N} \sum_{\vec{k}} \left( \frac{1}{1 + e^{\beta[\epsilon(\vec{k}) - \mu]}} + \frac{1}{1 + e^{\beta[E(\vec{k}) - \mu]}} \right), \quad (10)$$

we obtain Eq. (6b) from Eq. (10) in the same strong interaction limit. Thus, the model of Ref. 6 re-

duces to the one-dimensional lattice-gas model in this limit. One advantage of the lattice-gas model is that it has the same simple form in three dimensions as it has in one. This is because it can be easily seen that the parameter  $J(\vec{Q})$  is the same on all octahedral sites since it is, within a sign, the electrostatic potential seen by an extra electron on an octahedral site. This electrostatic potential has only the two values  $\pm J(\vec{Q})$  on  $\text{Fe}^{+3}$  and  $\text{Fe}^{+2}$  sites, as seen from the lattice structure (see Ref. 7). Callen and Cullen have extended their band model to three dimensions.<sup>10</sup> In three dimensions, because there are four octahedral-site atoms per unit cell, one must consider four bands. A second advantage of the lattice-gas model is that we need not specify whether band motion or small-polaron hopping is the correct description of the electronic states. The simplicity of the lattice-gas model makes it a suitable starting point for a phenomenological theory, which is able to tie together much of the experimental data on the metal-insulator transition in magnetite.

We may obtain  $T_c$  as a function of  $M$  by solving Eqs. (6a) and (6b) simultaneously, choosing  $H_m$  such that  $M$  remains constant as a function of  $T$ . When this is done,  $T_c$  (the temperature above which  $M'$  vanishes) is found to be given by

$$T_c \approx T_c^0 (1 - M^2) \quad \text{for } |M| \ll 1 \quad (11)$$

(to second order in  $|M|$ ). Thus  $T_c$  decreases with decreasing stoichiometry (i.e., with increasing  $|M|$ ) although the decrease is nowhere near as great as that observed experimentally.<sup>5</sup> Since  $T_c$  decreases with  $|M|$ , whether the number of electrons in the system is increased or decreased, we find that the lattice-gas model removes Rosen-cwaig's objection<sup>4</sup> to the Mott-Wigner model.  $T_c$  does decrease as the number of electrons is decreased. The physical reason for the decrease in  $T_c$  with decreasing stoichiometry is that added electrons fill in the sites on the  $\text{Fe}^{+3}$  ion rows and added holes fill in sites in  $\text{Fe}^{+2}$  rows, thus reducing the magnitude of the staggered molecular field [i.e.,  $J(\vec{Q})M'$ ], which is what holds the system in the ordered state.

When the system is completely ordered (i.e.,  $M' = 1$ ) and  $M = 0$  there can be no conduction by octahedral-site electrons because they are constrained to be in alternate-filled rows of octahedral sites. As  $M'$  decreases, however, the alternate rows of octahedral sites are neither completely ordered nor completely filled, and thus the system can conduct electricity. Therefore, as  $T$  approaches  $T_c$ , the conductivity should increase roughly as  $1 - M'$ . The increase is, however, not as rapid as observed experimentally.<sup>5</sup> Whereas the lattice-gas model gives a second-order phase transition, the transition in magnetite occurring at  $120^\circ$  is actually

first order.<sup>5</sup> Since the lattice-gas model does not give the observed first-order transition and since the decrease of  $T_c$  with  $|M|$  given by the lattice-gas model is nowhere near as great as the observed decrease,<sup>5</sup> it is necessary to modify our original model. There are two important effects which we have left out of our model which could account for the discrepancy, the screening of the interaction by free carriers and local polarization of nonoctahedral-site ions (particularly oxygen) around the ordered octahedral-site ions. Screening effects of free carriers can be accounted for by dividing the effective interaction  $J(\vec{Q})$  by a dielectric constant  $\kappa(\vec{Q})$  which increases with increasing number of free carriers, i. e., with  $1 - M'$ . Such a dielectric constant could result in a first-order transition.<sup>1</sup> Because of the magnitude of the screening necessary to explain the observed discontinuity in order parameter at  $T_c$ , however, it is quite likely that it is mainly the polarization of nonoctahedral-site ions that accounts for the sharpness of the first-order transition.

Nonoctahedral-site ions can be both displaced rigidly and polarized. The gap or excitation energy  $E_g^0 = J(\vec{Q})M'$  (i. e., the energy required to excite an electron from a site in an  $\text{Fe}^{+2}$  row to a site in an  $\text{Fe}^{+3}$  row) is essentially a mean electrical potential difference between octahedral sites in  $\text{Fe}^{+3}$  and  $\text{Fe}^{+2}$  rows as seen by an extra electron. Then, if  $d$  is the spacing between two adjacent ions in  $\text{Fe}^{+3}$  and  $\text{Fe}^{+2}$  rows,  $E_g/d$  is the average electric field between them. For simplicity, we will treat the charge density between these two atoms as a polarizable continuous medium. Then,

$$E_g/d = E_{g0}/d + f(p), \quad (12)$$

where  $f(p)$  is an unknown function of the polarization,  $p$  is the polarization of the medium, and  $E_{g0}$  is the gap in the absence of polarization, which is proportional to  $M'$ . Then,

$$E_g = E_{g0} + g(E_g), \quad (13)$$

where  $g(E_g) = f(p)d$  since  $p = p(E_g/d)$ . Here we have used the fact that  $p$  is a function of the average electric field. The gap can be a fairly nonlinear function of  $p$  because the oxygen atomic wave functions vary quite nonlinearly with distance from the nucleus of the atom.<sup>11</sup> Thus, a small displacement of the oxygen electronic charge can cause a large change in the potential difference between  $\text{Fe}^{+2}$  and  $\text{Fe}^{+3}$  sites. This is found to be so in calculating potentials for doing energy-band calculations.<sup>11</sup> This leads to nonlinear dependence of  $E_g$  on  $M'$ . For example, let

$$E_g = E_{g0} + \alpha E_g^2. \quad (14)$$

Then,

$$E_g = \frac{1}{2\alpha} - \left( \frac{1}{4\alpha^2} - \frac{E_{g0}}{\alpha} \right)^{1/2}. \quad (15)$$

For  $E_{g0}$  close to (but less than)  $1/4\alpha$ , the rate of change of  $E_g$  with  $E_{g0}$ , and hence  $M'$ , can be very large. This contribution to the gap energy due to local distortion or polarization is similar to that considered by Adler and Brooks<sup>12</sup> in their discussion of the metal-to-insulator transition. In their model, the lattice distortion alone gives rise to the phase transition, whereas in the model presented here the local lattice distortion or polarization is triggered by the Coulomb interaction.

In order to take into account the effect of both this local lattice polarization and screening effects of free carriers on the phase transition we will consider Eq. (6) with a gap energy that changes rapidly with  $M'$ . Since we do not know the precise form of the function  $g(E_g)$  in Eq. (13), we will choose a simple form for  $E_g$  as a function of  $M'$  having few parameters, such that  $E_g$  increases very rapidly with  $M'$  near  $M' = 1$ . We will choose the following form for simplicity

$$E_g = V_0 \left( \frac{D-1}{D-M'} \right) M', \quad (16)$$

where  $D$  is a constant  $>1$  and  $V_0$  is the gap energy at  $T=0$ . This form is not unique; there are many other forms that would be equally suitable for interpreting experiments, but this one is simple and has few parameters to be fit. We will take this  $E_g$  to replace  $J(\vec{Q})M'$  in Eq. (6). We can think of this as a substitution of an effective "dielectric constant" in Eq. (6), so that  $J(\vec{Q})$  is replaced by

$$V_0/\kappa(\vec{Q}), \quad (17)$$

where the dielectric constant  $\kappa(\vec{Q})$  is given by

$$\kappa(Q) = \frac{D-M'}{D-1}.$$

If screening due to free carriers were partly responsible for the first-order transition, it too would be accounted for phenomenologically by  $\kappa(\vec{Q})$  since  $\kappa(\vec{Q})$  used here increases with increasing number of free carriers.

If  $M$  is taken equal to zero, Eqs. (8) and (17) may be solved simultaneously to find  $M'$  as a function of temperature. When  $M=0$ , Eq. (6) becomes

$$M' = \tanh x, \quad (18a)$$

where

$$x = CM'/(D-M'), \quad (18b)$$

where

$$C = \beta V_0(D-1). \quad (18c)$$

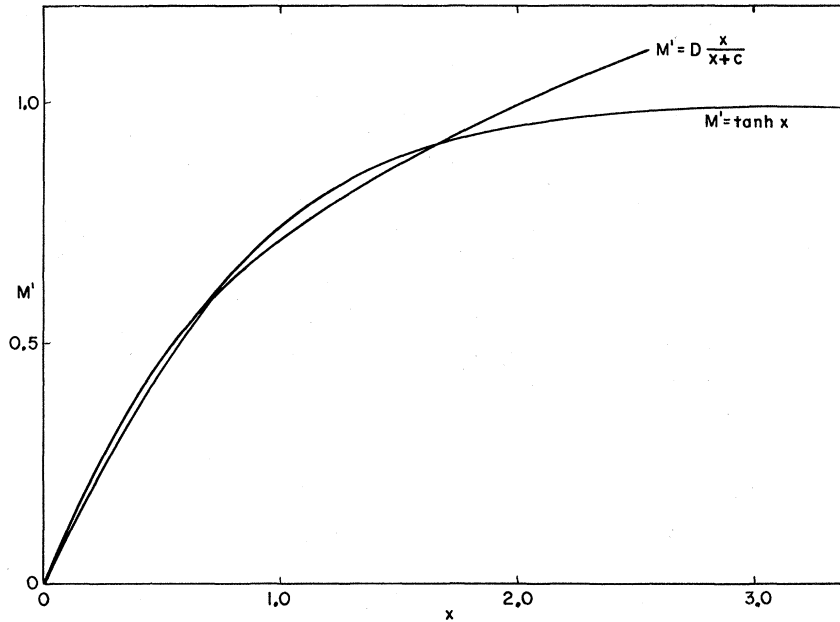


FIG. 2. Method of finding  $M'$  as a function of temperature is illustrated here. In this figure,  $D=1.5$  and  $C=1$ . Point of intersection of the two curves with the highest value of  $M'$  is the value of  $M'$  for that temperature (i. e., for that value of  $C$ ). ( $M'$  and  $x$  are dimensionless.)

If we solve Eq. (18b) for  $M'$ , we obtain

$$M' = Dx/(x+C). \quad (19)$$

To find  $M'$  as a function of temperature, we simply plot Eqs. (18a) and (19) as a function of  $x$  and look for points of intersection of the two curves, for various values of  $C$  (see Fig. 2). In ordinary molecular-field theory [which we obtain by erasing  $x$  in the denominator of Eq. (19)], Eq. (19) is a straight line and thus intersects Eq. (18a) at only two points.<sup>13</sup> In the case considered here, Eq. (19) bends over and intersects Eq. (18a) at three points. We take the solution with the largest value of  $M'$ , as it will give the lowest free energy. Above a certain temperature (i. e., below a certain value of  $C$ ), the curves only intersect at  $M'=0$ . Since just below this temperature  $M'$  is nonzero, the transition is first order, as predicted by Mott<sup>1</sup> and as observed experimentally<sup>5</sup> for magnetite. The simultaneous solution of Eqs. (18a) and (19) is illustrated in Fig. 1. As  $D$  gets closer to 1, the discontinuity of  $M'$  at the transition becomes greater, approaching 1 as  $D$  approaches 1 from above. Conversely, as  $D$  increases, the discontinuity in  $M'$  decreases. For large  $D$  it is possible to find the transition temperature analytically by expanding Eqs. (18a) and (19) to third order in  $x$  and solving the resulting cubic equation.

### III. INTERPRETATION OF EXPERIMENTAL RESULTS

Now let us use the phenomenological theory of Sec. II to interpret some experimental data.

Since the free energy in the screened molecular-field theory depends only on the order parameter  $M'$ , a discontinuous change in  $M'$  results in a dis-

continuous change in the free energy, or a sharp peak in the specific heat. A sharp peak in the specific heat of magnetite at the transition temperature is observed experimentally.<sup>14</sup>

When a small number of holes is added by doping  $\text{Fe}_3\text{O}_4$  with  $\text{Fe}_2\text{O}_3$ , the decrease of  $T_c$  with increasing number of excess carriers is found to be much greater than predicted by Eq. (11).<sup>5</sup> Let us now see if the effect of local lattice distortion and free-carriers screening, which are phenomenologically treated by Eqs. (18) and (19), will result in the sharp decrease of  $T_c$  with decreasing stoichiometry observed experimentally.<sup>5</sup> We use Eq. (6a) or (6b) with  $J(\vec{Q})M'$  replaced by  $E_g$  given by Eq. (16). Solving a quadratic equation for  $\tanh\beta H_m$  as a function of  $M$ , which is obtained by applying the well-known identity for  $\tanh(x \pm y)$  to Eq. (6b),

$$\tanh(x \pm y) = \frac{\tanh x \pm \tanh y}{1 \pm \tanh x \tanh y},$$

we obtain

$$\tanh\beta H_m = -\frac{1-\mu^2}{2M\mu^2} \pm \left[ \left( \frac{1-\mu^2}{2M\mu^2} \right)^2 + \frac{1}{\mu^2} \right]^{1/2}, \quad (20a)$$

where we take the plus sign for  $M > 0$  and the minus sign for  $M < 0$ , and where  $\mu = \tanh\beta E_g$ . Substituting in Eq. (6a), again using the identity for  $\tanh(x \pm y)$ , we find

$$M' = \mu \frac{1 - \tanh^2\beta H_m}{1 - \mu^2 \tanh^2\beta H_m}, \quad (20b)$$

and hence, when  $|M|$  is increased from 0 to 0.01 (corresponding to a 1% change in number of  $\text{Fe}^{+2}$  ions), Eq. (18a) should be replaced by

$$M' = (1 - 0.004)\tanh x.$$

As expected, it is found from Eqs. (20a) and (20b) that  $M'$  is a function of  $|M|$ , and hence is the same whether a given  $|M|$  corresponds to an increase in the number of electrons or a decrease below the number corresponding to perfect stoichiometry. Since a solution of Eqs. (18) and (19) will now occur when

$$Dx/(x+C) = (1 - 0.004)\tanh x,$$

we may take the effect of nonzero  $M$  into account by replacing  $D$  by  $D + \Delta D$ , where  $\Delta D = 0.004D \approx 0.004$  (since  $D$  will be close to 1 in this calculation).

The effect on  $T_c$  of adding carriers to the system will now be calculated by adding  $\Delta D = 0.004$  to  $D$  in Eq. (19). For any  $T \leq T_c$ , the values of  $M'$  given by Eqs. (18a) and (19) are equal. At  $T_c$  their slopes are also equal. Then

$$D[x/(x+C)] = \tanh x \quad (21a)$$

and

$$D[C/(x+C)^2] = \text{sech}^2 x. \quad (21b)$$

Although  $\Delta D$  (the perturbation in  $M'$  due to  $M$  being nonzero) depends on  $x$ , the dependence is small when  $M'$  is close to 1 and, therefore, we need not differentiate  $\Delta D$  with respect to  $x$  in Eq. (21b).

Taking differentials and setting  $dD = \Delta D$ , we obtain

$$[D - (x+C)\text{sech}^2 x - \tanh x]dx - \tanh x dC = -x\Delta D, \quad (22a)$$

$$(2DC \cosh x \sinh x - 2x - 2C)dx$$

$$+ (D \cosh^2 x - 2C - 2x)dC = -C \cosh^2 x \Delta D. \quad (22b)$$

Taking the values  $D = 1.04$ ,  $C = 0.05$ , and  $x = 2.65$ , which give the observed jump of  $M'$  by a factor of 100 at  $T = T_c$ , we obtain

$$dT_c/T_c = -dC/C = -24\Delta D = -24(0.004) = -0.10. \quad (23)$$

This equation gives a change of 10% in  $T_c$  for a 1% increase in the number of electrons or holes over the stoichiometric ratio (i.e., for  $M = 0.01$ ). These results are of the correct order of magnitude as the experimental results of Ref. 5. The  $T_c$  vs  $|M|$  curve is also found to be concave downwards as in Ref. 5.

As pointed out by Cullen and Callen,<sup>6</sup> if the order is not complete, the ordered state would correspond to a semimetallic rather than an insulating state. This occurs essentially because if the order is not complete, there are many carriers in the "wrong" rows of octahedral sites which are free to move up and down these rows, and thus which need not overcome the activation energy needed to get a carrier from one of the ordered rows to the next in or-

der to conduct. If this were the case, however, near the transition temperature there would be greater conductivity perpendicular to the  $C$  axis (i.e., along the ordered rows) than along the  $C$  axis, which is exactly opposite to what is actually found.<sup>15</sup> Since the conductivity below  $T_c$  is always greatest along the  $C$  axis, the system must be nearly completely ordered below the transition temperature, even near  $T_c$ . If the system is nearly completely ordered below  $T_c$ , it could turn out that the conductivity due to tunneling of carriers from a row of  $\text{Fe}^{+2}$  ions to a row of  $\text{Fe}^{+3}$  ions could be larger than the conductivity due to the few free carriers that already exist in "wrong rows" below  $T_c$ . This could give the observed result that the conductivity is greater along the  $C$  axis than perpendicular to it.<sup>15</sup> Therefore, the transition must be quite sharp. If the electrical conductivity is assumed to be proportional to  $1 - M'$ , Calhoun's data<sup>15</sup> indicate that  $M'$  must drop to zero from a value which is close to 99% of its zero-temperature value since the conductivity jumps by a factor of 100 at the transition temperature.

We will now look at the pressure dependence of the transition temperature. In order to discuss the dependence of  $T_c$  on pressure, it is necessary to include the electron kinetic or band energy. Therefore, the lattice-gas model that we have been using is not appropriate here. Hence, we will now use the one-dimensional energy-band model of Cullen and Callen.<sup>6</sup> To accomplish this, we will expand Eq. (8) to first order in the ratio of bandwidth to  $J(\vec{Q})$  at  $T = 0$  with  $\mu = 0$  (this corresponds to  $M = 0$ ). We find

$$M' \approx 1 - \frac{1}{N} \sum_{\vec{k}} \left[ 1 - \left( \frac{\epsilon(\vec{k}) - \epsilon(\vec{k} + \vec{Q})}{J(\vec{Q})} \right)^2 \right]. \quad (24)$$

Here, we will set  $J(\vec{Q})$  equal to  $E_g$  of Eq. (16) evaluated at  $M' = 1$ , its zero-temperature value. Pressure will increase the bandwidth by increasing interatomic overlap, and since the electron-electron interaction is usually not increased substantially by pressure, we see from Eq. (24) that pressure leads to a reduction in  $M'$  and thus an increase in conductivity. Since  $M'$  is reduced at  $T = 0$  by pressure, it is reasonable to assume that the transition temperature should be reduced, as is found experimentally.<sup>16</sup> Since the functional dependence of the bandwidth on pressure is not known, we will not proceed with a quantitative discussion of this effect. It should be noted, however, from Eq. (23), that because of the effective dielectric constant introduced here, a small reduction in  $M'$  caused by pressure, which, as was shown, is effectively accounted for by increasing  $D$ , can lead to a reduction in  $T_c$  20 times larger.

The choice of  $E_g$  in Eq. (16) is certainly not

unique. Other forms which produce a rapid increase of the molecular field with increasing  $M'$  yield similar results for the sharpness of the transition. For example, if  $E_g$  is taken proportional to  $M'^3$ , a first-order transition is also obtained. In this case, the discontinuity in  $M'$  at  $T_c$  is about 0.9.

#### IV. OPTICAL ABSORPTION AND INELASTIC NEUTRON SCATTERING IN ORDERED STATE

In this section we discuss the use of optical absorption and inelastic neutron scattering to check some of the predictions of the Verwey model of  $\text{Fe}_3\text{O}_4$ , to obtain elementary excitation energies, and to obtain experimental values of some of the parameters characterizing the ordered state. In the ordered state, the octahedral site  $\text{Fe}^{+3}$  and  $\text{Fe}^{+2}$  ions order in mutually perpendicular rows.<sup>7</sup> An elementary excitation of the system is obtained by taking an electron from an  $\text{Fe}^{+2}$  ion and placing it on a nearby  $\text{Fe}^{+3}$  ion. Because of the interaction between this electron and the hole left behind, there may be bound excitonic states.

To discuss the eigenstates of this system, we assume that the electron and hole created are able to move along their respective rows of  $\text{Fe}^{+3}$  and  $\text{Fe}^{+2}$  ions with their respective kinetic energies given by

$$p_{1x}^2/2m_1 \quad (25a)$$

and

$$p_{2y}^2/2m_2, \quad (25b)$$

where  $m_1$  and  $m_2$  are the effective masses of the electron and hole, respectively. Here, we take the  $x$  direction as the direction of the row of  $\text{Fe}^{+3}$  ions. The interaction between the electron and hole is given by

$$g/(c^2 + x_1^2 + y_2^2)^{1/2}, \quad (26)$$

where  $g$  is the coupling constant (i.e.,  $e^2$  divided by the dielectric constant) and where  $c$  is the distance along the  $C$  axis between two adjacent perpendicular rows. The coordinates are the coordinates in a Wannier-function representation used by Elliot<sup>17</sup> in his discussion of excitons in semiconductors. We now assume for simplicity that the radii of the exciton states are much larger than a lattice constant, and thus we neglect  $c$  compared to the exciton radius and invoke a continuum approximation like that used by Elliot<sup>17</sup> (i.e., we take the position vectors of the sites to be continuous variables). For simplicity, we take  $m_1 = m_2 = m^*$ . Now the effective exciton Hamiltonian in the Wannier-function representation is given by

$$H = (1/2m^*)(p_{1x}^2 + p_{2y}^2) - g/(x_1^2 + y_2^2)^{1/2}, \quad (27)$$

which is just a two-dimensional version of the hydrogen-atom Hamiltonian. If we look for eigen-

functions of the form

$$\psi(x_1, y_2) = [\mu(r)/r^{1/2}] e^{im\theta}, \quad (28)$$

where  $r$  and  $\theta$  are the polar coordinates [i.e.,  $r = (x_1^2 + y_2^2)^{1/2}$ ] and  $m$  is a positive or negative integer, we obtain the following radial equation:

$$\left( \frac{d^2}{dx^2} - \frac{m^2 - \frac{1}{4}}{x^2} + \frac{\nu}{x} - \frac{1}{4} \right) \mu(x) = 0, \quad (29)$$

where

$$x = \kappa r, \quad \nu = 1/\kappa a,$$

where

$$\kappa = (-2m^*E)^{1/2}/\hbar, \quad a = \hbar^2/gm^*.$$

This is the hydrogen-atom radial equation with  $l(l+1)$  replaced by  $m^2 - \frac{1}{4}$ .<sup>18</sup> This equation may be solved, like the ordinary hydrogen atom, using hypergeometric functions. We then obtain exciton states with energy given by

$$E_p = -\frac{1}{p^2} \frac{g}{2a} + E_0, \quad (30)$$

where  $E_0$  is the energy to create an unbound electron-hole pair, and where  $p$  is given by

$$p = \frac{1}{2} + |m| + m', \quad (31)$$

where  $m'$  is a positive integer. Unlike usual excitons, these excitons do not form a band labeled by a wave vector, because they are not free to move through the crystal but are bound to a particular pair of rows. This occurs because the exciton wave functions are centered around the intersection of a row of  $\text{Fe}^{+2}$  and a row of  $\text{Fe}^{+3}$  ions. Unbound electron-hole eigenstates can also be found in terms of hypergeometric functions following Elliot's treatment.<sup>17</sup> The solution that we have obtained is valid if

$$a \gg c.$$

Even if this relation is not satisfied, the solution should still be valid for large  $p$ , for which the radius of the exciton becomes large.

Following Elliot,<sup>18</sup> the optical-absorption and neutron-scattering cross sections are proportional to

$$E_p |\langle 0 | \alpha | p \rangle|^2 \delta(E_p - \hbar\omega), \quad (32)$$

where

$$\alpha = e^{i\vec{q} \cdot \vec{r}} \hat{\epsilon} \cdot \vec{p}$$

for optical absorption and

$$\alpha = \frac{1}{2} e^{i\vec{q} \cdot \vec{r}} \sigma^x$$

for neutron scattering. Here,  $\vec{q}$  is the photon wave vector or neutron-scattering vector,  $\vec{p}$  is the momentum operator,  $\hat{\epsilon}$  is the photon polarization vector, and  $\sigma^x$  is a Pauli spin matrix. We then obtain

$$\langle 0 | \alpha | p \rangle = \sum_{ij} M_q(\vec{R}_i - \vec{R}_j) e^{i\vec{q} \cdot \vec{R}_i} \Phi(\vec{R}_i, \vec{R}_j), \quad (33)$$

where  $\vec{R}_i$  and  $\vec{R}_j$  denote electron and hole positions, respectively,  $\Phi(\vec{R}_i, \vec{R}_j)$  is the exciton wave function in the Wannier-function basis, and

$$M_q(\vec{R}_i - \vec{R}_j) = \frac{1}{2} \int d^3r w^*(\vec{r} - \vec{R}_i + \vec{R}_j) e^{i\vec{q} \cdot \vec{r}} w(\vec{r}) \quad (34)$$

for neutron scattering since all spins are assumed up. Here,  $w(\vec{r})$  is a Wannier function. For optical absorption,

$$M_q(\vec{R}_i - \vec{R}_j) = \int d^3r w^*(\vec{r} - \vec{R}_i + \vec{R}_j) \hat{\epsilon} \cdot \vec{p} e^{i\vec{q} \cdot \vec{r}} w(\vec{r}). \quad (35)$$

We see from Eqs. (32)–(35) that although the absorption and neutron-scattering cross sections depend on the wave vector, the exciton lines should appear for all  $\vec{q}$  at the same energy given by Eq. (30). From Elliot's paper,<sup>17</sup> we see that both the neutron diffraction and optical absorption will behave in the following way as a function of energy: There will be a series of discrete excitons on the low-energy side of the spectrum. These will eventually form an energy-independent continuous cross section, as illustrated in Eq. (3.10) in Elliot's paper.<sup>17</sup> At still higher energies, the cross section will increase with an  $(E_0 - E)^{1/2}$  energy dependence which represents the continuum of unbound electron-hole pairs. From Eqs. (18) and (19), we find that if the discontinuity in  $M'$  at  $T_c$  is 0.99, the continuum occurs at an energy of about  $7KT_c$  or around 70 meV, which is in the infrared for optical absorption and is within the range of neutron energies. Because these are charge-transfer transitions, the optical absorption and inelastic-neutron-scattering cross sections are proportional to the square of an overlap matrix element  $M_q(\vec{R}_i - \vec{R}_j)$  which could reduce the cross section somewhat over that of usual exciton states. Unfortunately, there is no reliable way to estimate  $M_q(\vec{R}_i - \vec{R}_j)$ .

Observation of these excitons would serve as a measurement of the ratio of the dielectric constant and effective mass in magnetite. It would also allow us to estimate the energy of ordering of the  $\text{Fe}^{+3}$  and  $\text{Fe}^{+2}$  ions. Even if a tight-binding exciton theory, which might be more applicable to magnetite, were used, the result that the exciton energies are wave vector independent would still be valid. This result is simply a consequence of the lattice structure in the ordered state. The other results should still be qualitatively correct.

#### V. CONCLUSIONS

It appears that much of the present experimental data on the Mott-Wigner transition in magnetite can

be fit into a consistent picture based on a molecular-field electron-lattice-gas model with a phenomenologically screened molecular field. The reason for the extremely rapid change of excitation energy  $E_c$  with  $M'$  near  $M' = 1$  needed to explain the experimental results is still not completely understood. A more detailed calculation of the electronic states of the crystal is probably necessary to understand this phenomenon.

The experimental results that can be fit by this model include the observed first-order phase transition,<sup>5</sup> the specific-heat anomaly, the dependence of the transition temperature on stoichiometry,<sup>5</sup> and the Verwey ordering of  $\text{Fe}^{+3}$  and  $\text{Fe}^{+2}$  ions<sup>8</sup> in rows as observed by neutron diffraction.<sup>7</sup> The dependence of transition temperature on pressure cannot be explained with the lattice-gas model used here because kinetic or hopping energy is not included in the model. We have sketched how one might treat these results using the model of Cullen and Callen.<sup>6</sup> A similar treatment could probably be given using a small-polaron hopping model. In both cases, the functional dependence of hopping or band energy on pressure is required, and these functions are not known well enough to do a fit of experimental results quantitatively. The elementary excitation spectrum to be observed by optical absorption and neutron diffraction were also discussed.

Three experiments that remain to be done are inelastic neutron diffraction, optical-absorption measurements, and measurements of the anisotropy of the resistivity as a function of doping with  $\text{Fe}_2\text{O}_3$ . The former two will give information on the various parameters occurring in the theory and will test some predictions of Sec. IV of this paper. It should also be possible to determine the gap energy as a function of temperature in this way. Measurements of the anisotropy of the conductivity as  $\text{Fe}_2\text{O}_3$  is added to  $\text{Fe}_3\text{O}_4$  (i. e., as holes are added) will test out a prediction of the discussion in this paper that the phase transition occurs when enough free carriers are present to reduce the effective interaction sufficiently to make the ordered state unstable. Adding  $\text{Fe}_2\text{O}_3$  increases the number of such free carriers. If the transition occurs before the conductivity can become greater normal to the C axis than along it, this would indicate that adding carriers in this way and increasing the temperature have the same effect. Another useful experiment is a carefully done elastic-neutron-scattering experiment to determine whether or not the  $\text{Fe}^{+3}$  and  $\text{Fe}^{+2}$  ions are completely ordered just below  $T_c$ .

In this paper, it was assumed that the Coulomb repulsion of electrons plays a dominant role in bringing about the ordering. In addition, we speculated that there is probably also an accompanying distortion of the lattice which stabilizes the ordered state, by making the ionic potential more positive



near  $\text{Fe}^{+2}$  sites than near the  $\text{Fe}^{+3}$  sites. This stabilization lowers the electronic energy and increases the electronic excitation energy. This is to be contrasted with the Adler-Brooks mechanism<sup>12</sup> of the insulator-metal transition in which the transition is caused entirely by the splitting of the energy bands caused by the reduction of the lattice symmetry resulting from lattice distortion. Although this mechanism is present in the magnetite transition, the electronic interaction clearly plays a dominant role. If there is such a local polarization of the nonoctahedral-site ions, it could possibly be detected in a carefully done elastic-neutron-scattering experiment.

Recent elastic-neutron-diffraction experiments<sup>19</sup> have revealed peaks in addition to those predicted by the Verwey ordering. Recent Mössbauer data are consistent with these results.<sup>20</sup> Cullen and Callen have explained<sup>10</sup> these experiments by doing a three-dimensional energy-band calculation with four bands

and three order parameters. The extra neutron peaks imply that not all sites are equivalent within a single row of  $\text{Fe}^{+3}$  or  $\text{Fe}^{+2}$  sites. This could conceivably also be caused by some sort of local lattice distortion, but the Cullen and Callen mechanism appears to be simpler. There still remains the question of why such ordering should occur, which is not answered by either explanation. We have not considered these effects in this paper. In order for the ordering of Ref. 10 to exist, the ions cannot be completely ordered as predicted by Verwey.<sup>5,8</sup> Further theoretical and experimental investigation is clearly needed to straighten out these points.

#### ACKNOWLEDGMENTS

I would like to thank J. Goodenough and D. Adler for useful discussions. I would also like to thank L. Dworin for reading over the manuscript and making suggestions.

<sup>1</sup>N. F. Mott, *Advan. Phys.* **16**, 113 (1967); *Proc. Phys. Soc. (London)* **A62**, 416 (1949); N. F. Mott's comments following D. Adler, *Rev. Mod. Phys.* **40**, 714 (1968).

<sup>2</sup>D. Adler, in *Advances in Solid State Physics*, edited by F. Seitz, D. Turnbull, and H. Ehrenreich (Academic, New York, 1968), Vol. 21, p. 1.

<sup>3</sup>E. Wigner, *Proc. Faraday Soc.* **34**, 678 (1938); W. J. Carr, *Phys. Rev.* **122**, 1437 (1961); R. A. Coldwell-Horsefall and A. A. Maradudin, *J. Math. Phys.* **1**, 395 (1960).

<sup>4</sup>A. Rosencwaig, *Phys. Rev.* **181**, 946 (1969).

<sup>5</sup>E. J. W. Verwey and P. W. Haayman, *Physics* **8**, 979 (1941).

<sup>6</sup>J. R. Cullen and E. Callen, *J. Appl. Phys.* **41**, 879 (1970).

<sup>7</sup>W. C. Hamilton, *Phys. Rev.* **110**, 1050 (1958).

<sup>8</sup>E. J. W. Verwey, *Z. Krist.* **91**, 65 (1935).

<sup>9</sup>R. Brout, *Phase Transitions* (Benjamin, New York, 1965), p. 48.

<sup>10</sup>E. Callen and J. R. Cullen, *Phys. Rev. Letters* **26**, 236 (1971); private communication.

<sup>11</sup>F. Herman and S. Skillman, *Atomic Calculations* (Prentice-Hall, Englewood Cliffs, N. J., 1963), calculations for oxygen; P. DeCicco (private communication).

<sup>12</sup>D. Adler and H. Brooks, *Phys. Rev.* **155**, 826 (1967).

<sup>13</sup>C. Kittel, *Introduction to Solid State Physics* (Wiley, New York, 1961), p. 405.

<sup>14</sup>B. S. Ellefson and N. W. Taylor, *J. Chem. Phys.* **2**, 58 (1934).

<sup>15</sup>B. A. Calhoun, *Phys. Rev.* **94**, 1577 (1954).

<sup>16</sup>G. A. Samara, *Phys. Rev. Letters* **21**, 795 (1968).

<sup>17</sup>R. J. Elliot, *Phys. Rev.* **108**, 1384 (1957).

<sup>18</sup>A. Messiah, *Quantum Mechanics* (Wiley, New York, 1961), Vol. I, pp. 412-420.

<sup>19</sup>E. J. Samuelson, E. J. Bleeker, L. Dobrzynski, and T. Riste, *J. Appl. Phys.* **39**, 1114 (1968).

<sup>20</sup>R. S. Hargrove and W. Kundig, *Solid State Commun.* **8**, 303 (1970).

## Method of Executing the Tight-Binding Method of Energy-Band Calculation\*

J. Q. Bartling<sup>†</sup> and R. A. Craig<sup>‡</sup>

*University of California, Riverside, California 92502*

(Received 7 July 1969; revised manuscript received 26 August 1970)

This paper discusses a new technique for evaluating the matrix elements in tight-binding band calculations. The method employs an expansion of the crystal potential in reciprocal-lattice vectors and the atomic wave functions by a Fourier integral. The matrix elements are reduced to sums over the reciprocal lattice.

One of the difficulties associated with the tight-binding method of band-structure calculation is the evaluation of the matrix elements of the overlap

matrix and Hamiltonian matrix. These matrix elements are weighted sums of many-center overlap and potential integrals. When the wave functions